Synthesis and Characterization of Cu x S (x = 1−2) Nanocrystals Formed by the Langmuir−Blodgett Technique

ARTICLE *in* THE JOURNAL OF PHYSICAL CHEMISTRY C · SEPTEMBER 2014

Impact Factor: 4.77 · DOI: 10.1021/jp507355t

11 AUTHORS, INCLUDING:

Alexander Milekhin
Institute of Semiconductor Physics
57 PUBLICATIONS **283** CITATIONS
SEE PROFILE

A. K. Gutakovskii
Institute of Semiconductor Physics
225 PUBLICATIONS **1,936** CITATIONS
SEE PROFILE

E. E. Rodyakina
Institute of Semiconductor Physics
25 PUBLICATIONS **40** CITATIONS
SEE PROFILE

Dietrich R. T. Zahn
Technische Universität Chemnitz
773 PUBLICATIONS **6,421** CITATIONS
SEE PROFILE

THE JOURNAL OF PHYSICAL CHEMISTRY C

Article

pubs.acs.org/JPCC

Synthesis and Characterization of Cu_xS (x = 1−2) Nanocrystals Formed by the Langmuir−Blodgett Technique

Nikolay A. Yeryukov,*[,†,‡] Alexander G. Milekhin,[†,‡] Larisa L. Sveshnikova,[†] Tatyana A. Duda,[†] Lev D. Pokrovsky,[†] Anton K. Gutakovskii,[†,‡] Stepan A. Batsanov,[†] Ekaterina E. Rodyakina,[†,‡] Alexander V. Latyshev,[†,‡] and Dietrich R.T. Zahn[§]

[†]A.V. Rzhanov Institute of Semiconductor Physics, pr. Lavrentjeva, 13, 630090 Novosibirsk, Russia

[‡]Novosibirsk State University, Pirogov str. 2, 630090 Novosibirsk, Russia

[§]Semiconductor Physics, Technische Universität Chemnitz, D-09107 Chemnitz, Germany

ABSTRACT: Here, we present the results on the investigation of structural and vibrational properties of Cu_xS (x = 1−2) nanocrystals formed using the Langmuir−Blodgett technique. The synthesis requires deposition of high quality Langmuir−Blodgett films of copper behenates on a solid substrate (Si, Au, and Pt). The Langmuir−Blodgett film is then sulfidized, what results in the formation of the copper sulfide nanocrystals embedded in behenic acid matrix. Finally, free-standing Cu_xS nanocrystals are obtained after temperature annealing at 120−400 °C in an Ar atmosphere. Morphology (size, shape, and areal density) and the crystal structure of nanocrystals were determined by direct structural methods including scanning and transmission electron microscopies and high-energy electron diffraction. Surface-enhanced Raman scattering (SERS) by optical phonons in Cu_xS nanocrystals in the vicinity of metal nanoclusters provided a significant enhancement factor (about 25) and allowed the fine structure of their phonon spectrum to be observed. SERS spectra of Cu_xS nanocrystals under annealing reveal the high frequency shift of optical phonon modes from 475 to 492 cm^{-1}, which is explained by the existence of minor copper-deficient crystal phases. The combination of surface-enhanced Raman scattering spectroscopy, electron diffraction, and electron transmission microscopy allowed us to establish at least three stable phases: CuS, $Cu_{1.8}S$, and Cu_2S.

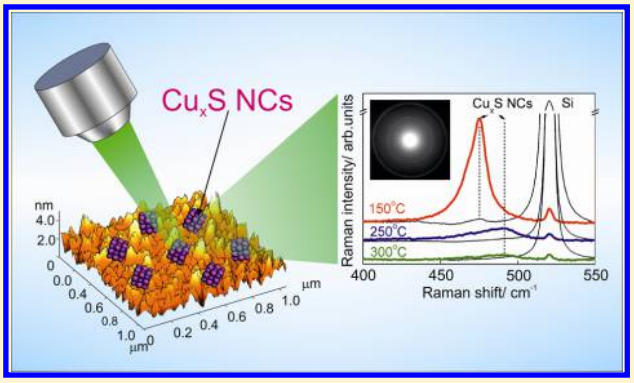

1. INTRODUCTION

Copper sulfides (Cu_xS) having unique physical properties (superionic conductivity,[1] superconductivity,[2] or p-type conductivity[3]) are considered by many researchers as promising materials for solar cells,[4−6] gas sensors,[7] switches,[8] and plasmonic applications.[9,10] It is well-known that Cu_xS possesses at least seven stable crystal modifications (with x = 2, 1.96, 1.8, 1.75, 1.32, 1.12, and 1) at room temperature.[11] This allows the properties of Cu_xS to be tuned in a broad range. In particular, the band gap of Cu_xS has values from 1.2 eV for the "copper-rich" phase Cu_2S to 2 eV for "copper deficient" CuS.[11,12]

More interesting physical properties of Cu_xS should appear if it is presented as nanoscale structures, in particular, nanocrystals (NCs) which reveal quantum confinement effects. Nowadays, there is a number of different methods to form Cu_xS NCs including wet[13] and colloid[14,15] chemistry, sonochemical[16] and hydrothermal[17] approaches yielding spherical, platelet-shaped, rod-, flake-, and flower-like NCs. Among others, the Langmuir−Blodgett (LB) technique[18] proved itself as a relatively fast, flexible, and low-cost method which enables semiconductor NCs of various composition, including Cu_xS NCs, and metal nanoclusters[19] to be synthesized. The structural parameters of the variety of the NCs were established by a combination of direct structural methods such as high resolution and scanning electron microscopies, atomic-force microscopy, and reflection high energy electron diffraction.[20,21]

One of the most efficient optical methods suitable for the determination of phase composition of different materials including nanoscale Cu_xS is Raman spectroscopy. However, only copper-deficient Cu_xS phases (with x < 1.4) have covalent S−S bonds, the stretching vibrations of which can be detected by Raman spectroscopy. Indeed, the group theoretical analysis predicts eights Raman active phonon modes for CuS: $2A_{1g}$, $2E_{1g}$, and $4E_{2g}$.[22] Three intense phonon modes at about 20, 60, and 475 cm^{-1} and three weaker bands at 115, 140, and 265 cm^{-1} are typically observed in the Raman spectra of CuS. The modes near 20 and 475 cm^{-1} are assigned to vibrational modes from the covalent S−S bonds. The latter is the most intensive and the frequently observed mode in Raman experiments. The other modes are assigned to bending and lattice vibrational

Received: July 23, 2014
Revised: September 4, 2014
Published: September 29, 2014

modes. Even though the Cu−S system was investigated in terms of Raman scattering by different researchers, their data are inconsistent with each other. For instance, it was reported[23] that the Raman spectra of Cu_2S and CuS thin films reveal characteristic Raman phonon modes at frequencies of 472 and 474 cm^{-1}, respectively, while the Raman study of Cu_2S, $Cu_{1.8}S$, $Cu_{1.12}S$, and CuS[24] provides corresponding values at 465, 466, 470, and 474 cm^{-1}. Moreover, the phonon mode observed at 462 cm^{-1} was assigned to the lattice vibrations of CuS.[25] Contrary to these results, Safrani et al.[26] stated that CuS and $Cu_{1.8}S$ are undistinguishable by means of Raman spectroscopy. Parker et al.[27] concluded that Raman spectroscopy allows copper sulfides to be classified into two groups only, namely with S−S bonds and without them, but within each group the Raman spectra show no difference. As it can be seen, the lack of agreement of experimental data is apparent and the mode frequency spread even for stoichiometric CuS is more than 10 cm^{-1}. Another challenge is that the Raman cross section in copper-deficient Cu_xS and, thus, the Raman response is in a many time lower compared to that in CuS. This fact complicates the acquirement and the analysis of Raman data. As recently reported by Milekhin et al.,[28] the phonon spectrum of NCs can be successfully studied using the surface enhanced Raman scattering (SERS) effect. This phenomenon consists in a drastic increase of Raman scattering by semiconductor NCs formed in the vicinity of rough metal surfaces or metal nanoclusters. SERS is caused by a strong enhancement of the electromagnetic field E near the metal clusters when optically excited with a photon energy close to the surface plasmon resonance energy. SERS is suitable for enhancing confined and surface optical phonon modes in different semiconductor NCs including CdSe,[29] CdS,[28] ZnO,[30] and CuS[31] formed in the vicinity of metal (Au or Pt) nanoclusters. Therefore, application of SERS for probing a vibrational spectrum in copper-deficient Cu_xS NCs seems to be very promising for the characterization of their crystal structure.

In this study, the interconnection of structural, optical, and vibrational properties of Cu_xS (x = 1−2) NCs prepared by Langmuir−Blodgett technique is established by a combination of results from transmission and scanning electron microscopies, electron diffraction, and surface enhanced Raman scattering.

2. EXPERIMENTAL SECTION

Cu_xS NCs were obtained by means of the Langmuir−Blodgett technique.[18] Briefly, at the first stage, a behenic acid dissolved in hexane was spread onto the water surface in a LB bath using a $CuSO_4$ solution as a subphase. The copper behenate films formed were then transferred (Y-type) from the water surface onto a bare silicon substrate or one covered with Au or Pt nanocluster films. The typical thickness of copper behenate films was 200 monolayers (MLs). For electron microscopy and diffraction (transmission mode) measurement, 10−30 ML thick LB films were formed on carbon-coated Au grids. At the second stage, the nucleation of Cu_xS nanoclusters in the organic matrix took place by sulfidizing the structure. The existence of Cu_xS nanoclusters with an average size of 3 nm and areal density of 10^{11} cm^{-2} formed in the organic matrix was confirmed by high-resolution transmission electron microscopy (HRTEM).[32] Because of the small size of Cu_xS nanoclusters, establishing their crystallinity is hardly possible by HRTEM. At the last stage, 4 h annealing in a temperature range of 120−400 °C in an Ar atmosphere resulted in the removal of the matrix and the formation of free-standing Cu_xS NCs on a solid substrate (bare Si, Au, and Pt). Au and Pt nanocluster films with effective thicknesses of 40−100 and 100 nm, respectively, were formed on Si (001) by means of evaporation in ultrahigh vacuum and were used as substrates for depositing NC films for further SERS experiments.

The size, shape, and areal density of Cu_xS NCs were determined using scanning electron microscopy (SEM) and HRTEM. SEM images were acquired using a Raith-150 system at 10 kV acceleration voltage, 30 μm aperture, and 6 mm working distance.

The morphology of the metal nanocluster films was determined by atomic force microscopy (AFM). AFM measurements were performed with a Solver P47-H (NT-MDT) atomic force microscope operating in semicontact topography mode using silicon cantilevers with resonant frequencies in the range of 100−250 kHz providing the vertical resolution better than 0.1 nm and lateral resolution of 7−10 nm.

HRTEM images were recorded using a Titan 80-300 (FEI) electron microscopy operating in scanning transmission electron microscopy (STEM) and HRTEM modes at 300 kV acceleration voltage.

Reflection and transmission high-energy electron diffraction measurements were carried out with a EF-Z4-Z5 setup and BS-513A at the 50 and 100 kV acceleration voltages, respectively.

Micro-Raman experiments were performed with Jobin Yvon Dilor XY800, T64000, and LabRam-UV spectrometers in backscattering geometry at 300 and 77 K. A set of excitation lines of Ar^+, Kr^+, HeCd lasers ranging from 325 to 725.5 nm was used. The laser light incident on a sample surface was focused to a 1 μm spot diameter with the power of about 2 mW.

3. RESULTS AND DISCUSSION

3.1. Microscopy Analysis. Figure 1 shows typical HRTEM images of Cu_xS NCs annealed at 150, 250, and 300 °C in an Ar atmosphere. Analysis of the HRTEM images allows both morphology and crystal structure changes upon annealing to be established. Annealing of pristine Cu_xS nanocluster samples at temperatures in the range of 150−200 °C results in the formation of round-shape NCs with average size of about 7 nm and with crystal structure corresponding to CuS. Increasing the annealing temperature to 200 °C causes the coalescence of some CuS NCs into conglomerates with dimensions of 20−60 nm. In addition to the CuS phase, Cu_2S is formed by further increasing the annealing temperature above 250 °C. Upon temperature annealing in the range of 120−400 °C, the crystals reveal a hexagonal symmetry. A more detailed HRTEM analysis of Cu_xS NCs was performed by Gutakovskii et al.[32]

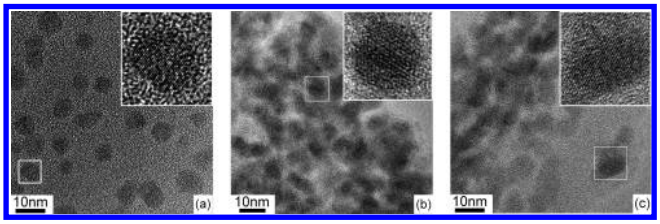

Figure 1. Typical HRTEM images of Cu_xS annealed at (a) 150, (b) 250, and (c) 300 °C.

dx.doi.org/10.1021/jp507355t | J. Phys. Chem. C 2014, 118, 23409−23414

The uniformity of the CuS NCs (10 MLs) distributed over the surface of bare Si and that covered with Au and Pt nanoclusters as well as the morphology of the metal nanoclusters was investigated by SEM. As can be seen in Figure2, a uniform coverage is observed for CuS NCs deposited

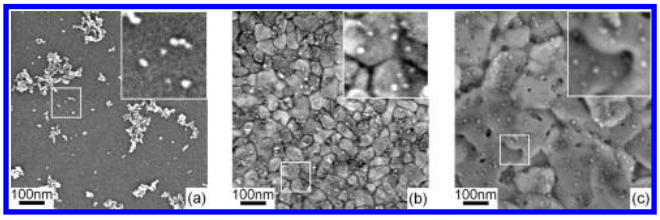

Figure 2. Typical SEM images of sample with CuS NCs fabricated on (a) Si, (b) Au, and (c) Pt surfaces, respectively, after annealing at 150 °C.

on the metal surfaces, whereas CuS NCs on Si form conglomerates with a size up to 100 nm. However, the average areal density of the NCs is nearly the same for all samples and amounts to 1.2×10^{11}cm^{-2} (accuracy of 5%).

Furthermore, SEM images obtained allow lateral sizes of Au and Pt nanoclusters to be estimated. These are 20−50 and 50−150 nm, respectively. The height roughness of Au and Pt nanocluster films is determined from AFM images presented in Figure 3. As it can be seen from this figure, the Au and Pt nanocluster heights are about 5 and 25 nm, respectively.

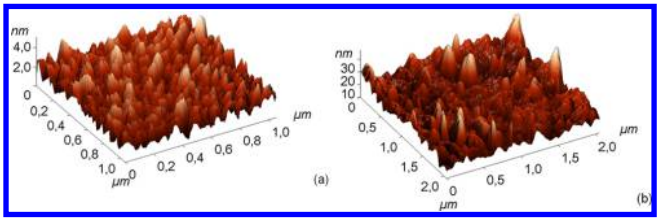

Figure 3. Typical AFM images of (a) Au and (b) Pt nanocluster surfaces.

3.2. Diffraction Analysis. Phase composition and crystal symmetry of Cu$_x$S NCs were determined by using high-energy electron diffraction. Typical electron diffraction patterns of the samples annealed at 150, 250, and 400 °C are presented in Figure 4. The diffuse character of the Debye rings in the diffraction pattern of the sample annealed at 150 °C (Figure 4a) resulted from extremely small size (less than 10 nm) of NCs. Annealing of the samples at higher temperatures (from 250 to 400 °C) leads to the appearance of more defined rings (Figure 4b,c), which evidence the increasing NC size. It is worth mentioning that in the case of the sample annealed at 250 °C the diffraction pattern (Figure 4b) was recorded in a transmission mode, which turned out to be more informative than the reflection one (not shown in the figures).

The comparison of experimental interplanar distances and relative intensities of the rings derived from the diffraction patterns with those of JCPDS reference data[33] is summarized in Table 1. In the table, d_I denotes the interplanar distance expressed in angstroms with a corresponding relative intensity presented as subscript I. Thus, 3.285_{14} should be read as a diffraction ring corresponding to an interplanar distance of 3.285 Å with relative intensity of 14 counts. The subscript related to the experimental interplanar distances indicates intensity qualitatively in terms of medium (m.), weak (w.), and

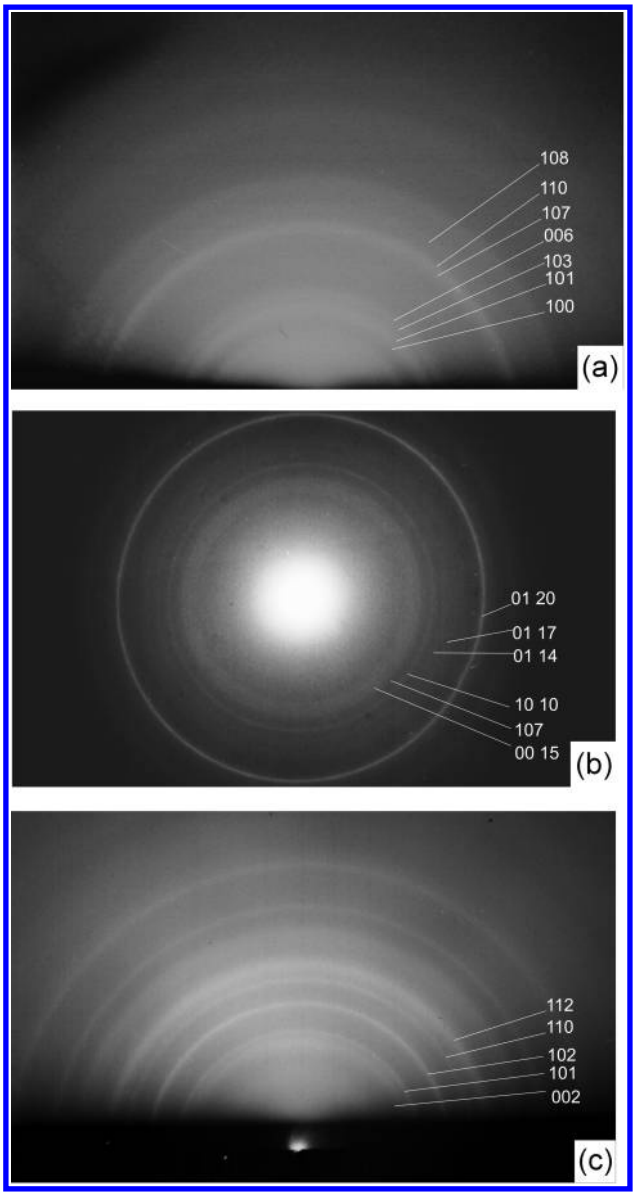

Figure 4. Typical diffraction patterns of the samples with Cu$_x$S NCs annealed at (a) 150, (b) 250, and (c) 400 °C. The indexing is taken from ref 32

very weak (v.w.). Reference *hkl* indices of corresponding planes are presented in the table as well. From the table one can see that basic reflexes agree well with those of reference data; however, some differences of experimental and reference intensities occur. Using the reference data of bulk monocrystal, whereas samples under investigation belong to the nanoscale, can be supposed to be a reasonable explanation of this mismatch.

Hence, it was established that annealing under 150 °C leads to the formation of CuS NCs of hexagonal ($P6_3/mmc$) symmetry with lattice constants a = 3.792 Å and c = 16.43 Å. An increase of annealing temperature up to 250 °C causes transformation of CuS to $C_{1.8}S$ of rhombohedral ($R\bar{3}m$) symmetry with lattice constants a = 3.930 Å, c = 48.14 Å. With further annealing up to 400 °C the phase of hexagonal ($P6_3/mmc$) Cu_2S with lattice constants a = 3.95 Å, c = 6.75 Å appeared. The conclusions regarding crystal symmetry of the Cu$_x$S NCs derived from the diffraction measurements correlate

dx.doi.org/10.1021/jp507355t | J. Phys. Chem. C 2014, 118, 23409−23414

Table 1. Comparison of Experimental Diffraction Data of Cu_xS NCs Annealed at 150, 250, and 400 °C with the Reference Data

CuS (PDF 06−0464)	d_I(Å)	3.285_{14}	3.22_{30}	2.813_{100}	2.724_{55}	1.902_{25}	1.896_{75}	1.735_{35}
	hkl	100	101	103	006	107	110	108
Sample annealed at 150 °C	d_I(Å)	$3.33-3.18_{m.}$		$2.86-2.70_{w.}$		$1.96-1.89_{m.}$		$1.79_{w.}$
$Cu_{1.8}S$ (PDF 47−1748)	d_I(Å)	3.21_{46}	3.051_{11}	2.781_{46}	2.419_{5}	2.175_{7}	1.964_{100}	
	hkl	00 15	107	10 10	01 14	01 17	01 20	
Sample annealed at 250C°C	d_I(Å)	3.18_{w}	$3.04_{v.w.}$	2.64_{m}	$2.44_{v.w.}$	$2.2_{v.w.}$	$1.92_{m.}$	
Cu_2S (PDF 23−0961)	d_I(Å)	3.375_{16}	3.051_{97}	2.403_{100}	1.975_{71}	1.7046_{37}		
	hkl	002	101	102	110	112		
Sample annealed at 400 °C	d_I(Å)	$3.32-3.25_{w.}$	$3.01_{m.}$	$2.44-2.12_{m.}$	$1.96-1.91_{m.}$	$1.68-1.61_{w.}$		

with the HRTEM data described above and were further used for the analysis of the Raman data.

3.3. Raman Scattering. For the investigation of the phonon spectrum of Cu_xS NCs, Si substrates covered with Au and Pt nanocluster films (so-called SERS substrates) with Cu_xS NCs deposited by the LB technology were applied. The presence of rough surfaces allows the localized plasmon resonance to be exited, which can result in an enhancement of Raman scattering by Cu_xS NCs. The enhanced Raman scattering allows a detailed analysis of the phonon spectrum of Cu_xS NCs upon annealing to be performed. The efficiency of the SERS substrates in the case of Cu_xS NCs (200 MLs) annealed at 120 °C is demonstrated in Figure 5. The Raman

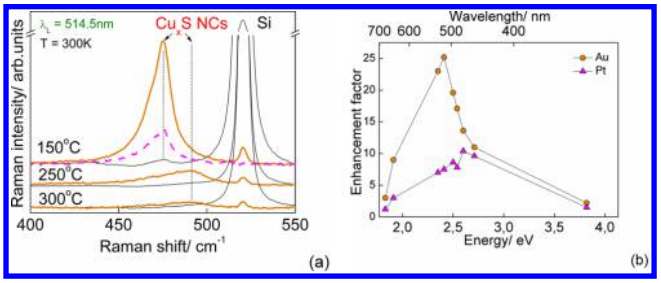

Figure 5. (a) Raman spectra of Cu_xS NCs annealed at 150, 250, and 300 °C on bare Si (thin solid lines), Au (thick solid lines), and Pt (dashed line) nanocluster film surfaces; (b) dependence of the enhancement factor for CuS NCs annealed at 150 °C formed on Au (circles) and Pt (triangles) nanocluster films on the excitation energy.

spectrum of the NCs formed on bare Si reveals a weak band near 475 cm^{-1}, which can be ascribed to the S−S stretching vibrations in crystalline CuS.[22] Here and further, the mode frequency positions were determined from the best fit of the experimental spectra with Lorentzian curves. The additional band observed near 521 cm^{-1} corresponds to the optical phonon mode of Si substrate. A significantly stronger signal of the mode near 475 cm^{-1} is observed in the Raman spectra of CuS NCs deposited on Au and Pt nanocluster films (Figure 5a) as expected for the SERS effect. Moreover, by tuning the excitation energy to that of the local surface plasmon, optimal resonance conditions can be realized. The SERS profile, that is, the dependence of the enhancement factor (EF) on excitation wavelength, obtained for CuS NCs on Au and Pt nanocluster films is shown in Figure 5b. The SERS profile reveals a resonance behavior with an EF maximum (factor of 25) at 2.41 eV for CuS NCs on Au nanocluster films. The maximum of the SERS profile for CuS NCs on Pt films is shifted to higher energy in accordance with the energy position of the localized plasmon resonance, which is expected for Pt in the blue spectral range. It is worth mentioning that the absence of this band in the spectra recorded for NCs deposited on a bare Si substrate annealed at 250 and 300 °C prevents the determination of the enhancement factor in the case of $Cu_{1.8}S$ and Cu_2S NCs. Optimized SERS conditions were further used for studying the phonon spectra of Cu_xS NCs deposited on an Au nanocluster surface. SERS spectra of Cu_xS NCs annealed at different temperatures and measured at 300 K are presented in Figure 6a. To avoid the heating effect and to obtain more detailed

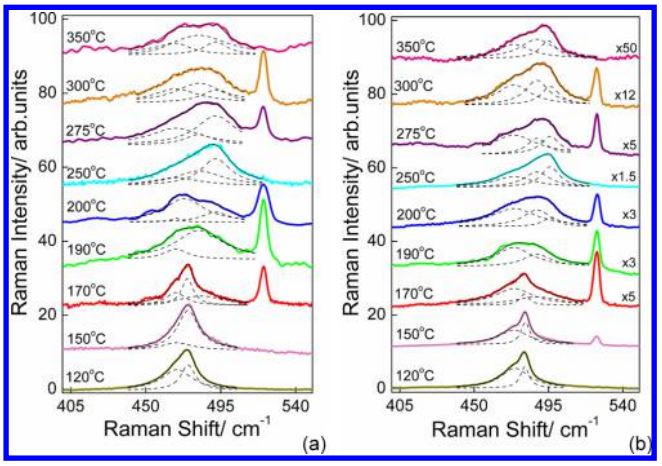

Figure 6. SERS spectra of Cu_xS NCs annealed at different temperatures, recorded with an excitation wavelength of 514.5 nm at (a) 300 and (b) 77 K.

information on the phonon modes in Cu_xS NCs, Raman measurements were carried out at 77 K (Figure 6b) as well. It is worth mentioning that the phonon modes are more prominent at low temperature and upward shifted by about 5 cm^{-1}. The spectra of the sample annealed at 120 °C taken at 300 (77) K reveal a prominent S−S band near 475 (480) cm^{-1}. This band possesses an asymmetric shape resulting from a weak shoulder at 468 (473) cm^{-1}. Note that the presence of this shoulder is found in all Raman spectra of Cu_xS NCs. The nature of the shoulder is rather unknown and it appears as a result of either vacancies in the CuS lattice[34] or thermal distortion of S−S bonds as it happens in elemental sulfur.[35] The strongest mode (475 (480) cm^{-1}) broadens, decreases in intensity with increasing annealing temperature, and finally is smeared out upon annealing at 190 °C (Figure 6b). Moreover, two new modes (about 483 (488) cm^{-1} and 492 (496) cm^{-1}) appear consequently at annealing temperatures of 170 and 200 °C, respectively. The intensity of these modes is drastically decreased (factor of 50) with increasing annealing temperature. It is very probable that the observation of these modes becomes

dx.doi.org/10.1021/jp507355t | J. Phys. Chem. C 2014, 118, 23409−23414

possible only due to the SERS effect. To the best of our knowledge, no information on the phonon modes in Cu_xS NCs having frequencies above 480 cm^{-1} is available in literature. Note that occasional changes of Si phonon mode intensity observed in the Raman spectra indicate an inhomogeneous Au film thickness.

Obviously the annealing of CuS NCs leads to the removal of sulfur atoms and the formation of a dominant phase of copper-rich sulfides with a minor phase of copper-deficient Cu_xS as confirmed by the diffraction measurements. Unlikely to copper-rich Cu_xS (x = 2, 1.8), copper-deficient sulfide NCs (with x < 1.4) can contribute to their Raman spectra, the S−S stretching mode which is Raman active. Only three Cu_xS compounds (with x = 1, 1.12, and 1.32) satisfy this condition and, therefore, only their presence can be evidenced from Raman spectra despite the dominant phase being a copper-rich sulfide. It is known from literature data[36,37] that the frequency position of the S−S bond vibration depends on the bond length and can vary in the frequency range from 474 to about 550 cm^{-1} with decreasing bond length.

Based on the literature data we assign the vibrational modes observed at 483 (488) cm^{-1} and 492 (496) cm^{-1} in the Raman spectra of Cu_xS NCs subjected to temperature annealing to the S−S stretching vibrations in copper-deficient sulfides with x = 1.12 and 1.32, respectively, or in metastable phases of copper-deficient Cu_xS having S−S bonds with the bond lengths lower than those in CuS.

CONCLUSION

Cu_xS NCs were synthesized using the LB technique with subsequent sulfidation and thermal annealing. The size, shape, and crystal structure of NCs were determined from HRTEM and RHEED experiments. The SERS effect by vibrational modes in NCs allows a detailed analysis of phonon spectrum of Cu_xS NCs formed in the temperature range from 120 to 350 °C to be performed. New phonon modes attributed to the S−S stretching vibrations in copper-deficient Cu_xS NCs were observed upon annealing at temperatures above 150 °C. Combining HRTEM, RHEED, and SERS spectroscopy, it is established that thermal annealing of pristine Cu_xS nanoclusters in LB films at temperatures of 120−150, 250, and 350−400 °C results in the formation of Cu_xS NCs having at least three major stable phases: CuS, $Cu_{1.8}S$, and Cu_2S and minor phases of copper-deficient Cu_xS NCs.

AUTHOR INFORMATION

Corresponding Author

*E-mail: yeryukov@isp.nsc.ru. Phone: 7(383)316-60-54. Fax:7(383)333-27-71.

Notes

The authors declare no competing financial interest.

ACKNOWLEDGMENTS

This study was supported by the Russian Foundation for Basic Research (project nos. 13-02-00063_a), the Siberian Branch of Russian Academy of Sciences (project SB RAN No. 134), and the German Research Society (Deutsche Forschungsgemeinschaft Grant No. Za146/22-1, Grant No. GRK 1215 "Materials and Concepts for Advanced Interconnects") and the Ministry of Education and Science of the Russian Federation.

REFERENCES

(1) Konev, V. N.; Chebotin, V. N.; Fomenkov, S. A. Diffusion phenomena in nonstoichiometric copper sulfide and selenide. *Inorg. Mater.* **1985**, *21*, 205−209.
(2) Mazin, I. I. Structural and electronic properties of the two-dimensional superconductor CuS with $1^1/_3$-valent copper. *Phys. Rev. B* **2012**, *85*, 115133.
(3) Nair, M. T. S.; Nair, P. K. Chemical bath deposition of Cu_xS thin films and their prospective large area applications. *Semicond. Sci. Technol.* **1989**, *4*, 191−199.
(4) Te Velde, T. S. The production of the cadmium sulphide-copper sulphide solar cell by means of a solid-state reaction. *Energy Convers.* **1975**, *15*, 111−115.
(5) Mane, R. S.; Lokhande, C. D. Chemical deposition method for metal chalcogenide thin films. *Mater. Chem. Phys.* **2000**, *65*, 1−31.
(6) Liu, G.; Schulmeyer, T.; Brötz, J.; Klein, A.; Jaegermann, W. Interface properties and band alignment of Cu_2S/CdS thin film solar cells. *Thin Solid Films* **2003**, *431 −432*, 477−482.
(7) Sagade, A. A.; Sharma, R. Copper sulphide (Cu_xS) as an ammonia gas sensor working at room temperature. *Sens. Actuators, B* **2008**, *133*, 135−143.
(8) Sakamoto, T.; Sunamura, H.; Kawaura, H.; Hasegawa, T.; Nakayama, T.; Aonob, M. Nanometer-scale switches using copper sulfide. *Appl. Phys. Lett.* **2003**, *82*, 3032−3034.
(9) Hsu, S.-W.; Bryks, W.; Tao, A. R. Effects of carrier density and shape on the localized surface plasmon resonances of $Cu_{2-x}S$ nanodisks. *Chem. Mater.* **2012**, *4*, 3765−3771.
(10) Zhao, Y.; Pan, H.; Lou, Y.; Qiu, X.; Zhu, J.; Burda, C. Plasmonic $Cu_{2-x}S$ nanocrystals: optical and structural properties of Copper-Deficient Copper(I) Sulfides. *J. Am. Chem. Soc.* **2009**, *131*, 4253−4261.
(11) Goble, R. J. The relationship between crystal structure, bonding, and cell dimensions in the coppers sulfides. *Can. Mineral.* **1985**, *23*, 61−76.
(12) Klimov, V. I.; Haring-Bolivar, P.; Karavanskii, V. A. Optical nonlinearities and carrier trapping dynamics in CdS and Cu_xS nanocrystals. *Superlattices Microstruct.* **1996**, *20*, 395−404.
(13) Kuzuya, T.; Itoh, K.; Ichidate, M.; Wakamatsu, T.; Fukunaka, Y.; Sumiyama, K. Facile synthesis of nearly monodispersed copper sulfide nanocrystals. *Electrochim. Acta* **2007**, *53*, 213−217.
(14) Silvester, E. J.; Grieser, F.; Sexton, B. A.; Healy, T. W. Spectroscopic studies on copper sulfide sols. *Langmuir* **1991**, *7*, 2917−2922.
(15) Xie, Y.; Riedinger, A.; Prato, M.; Casu, A.; Genovese, A.; Guardia, P.; Sottini, S.; Sangregorio, C.; Miszta, K.; Ghosh, S.; et al. Copper sulfide nanocrystals with tunable composition by reduction of covellite nanocrystals with Cu^+ ions. *J. Am. Chem. Soc.* **2013**, *135*, 17630−17637.
(16) Wang, H.; Zhang, J.-R.; Zhao, X.-N.; Xu, S.; Zhu, J.-J. Preparation of copper monosulfide and nickel monosulfide nanoparticles by sonochemical method. *Mater. Lett.* **2002**, *55*, 253−258.
(17) Ji, H.; Cao, J.; Feng, J.; Chang, X.; Ma, X.; Liu, J.; Zheng, M. Fabrication of CuS nanocrystals with various morphologies in the presence of a nonionic surfactant. *Mater. Lett.* **2005**, *59*, 3169−3172.
(18) Milekhin, A.; Sveshnikova, L.; Duda, T.; Surovtsev, N.; Adichtchev, S.; Ding, L.; Zahn, D. R. T. Vibrational spectra of quantum dots formed by Langmuir−Blodgett technique. *J. Vac. Sci. Technol., B: Microelectron. Nanometer Struct.−Process., Meas., Phenom.* **2010**, *28*, C5E22−C5E24.
(19) Surovtsev, N. V.; Adichtchev, S. V.; Duda, T. A.; Pokrovsky, L. D.; Sveshnikova, L. L. New surface-enhanced Raman scattering active substrate fabricated by use of the Langmuir−Blodgett technique. *J. Phys. Chem. C* **2010**, *114*, 4803−4807.
(20) Phuruangrat, A.; Thongtem, S.; Thongtem, T. Microwave hydrothermal synthesis and characterization of copper sulfide with different morphologies. *Chalcogenide Lett.* **2013**, *10* (10), 359−365.
(21) Protasov, D. Yu.; Jian, W.-B.; Svit, K. A.; Duda, T. A.; Teys, S. A.; Kozhuhov, A. S.; Sveshnikova, L. L.; Zhuravlev, K. S. Formation of

arrays of free-standing CdS quantum dots using the Langmuir-Blodgett technique. *J. Phys. Chem. C* **2011**, *115*, 20148−20152.
(22) Ishii, M.; Shibata, K.; Nozaki, H. Anion distributions and phase transitions in $CuS_{1-x}Se_x$ (x = 0−1) studied by Raman spectroscopy. *J. Solid State Chem.* **1993**, *105*, 504−511.
(23) Minceva-Sukarova, B.; Najdoski, M.; Grozdanov, I.; Chunnilall, C. J. Raman spectra of thin solid films of some metal sulfides. *J. Mol. Struct.* **1997**, *410*−*411*, 267−270.
(24) Kumar, P.; Nagarajan, R. An Elegant Room Temperature Procedure for the Precise Control of Composition in the Cu−S System. *Inorg. Chem.* **2011**, *50*, 9204−9206.
(25) Li, F.; Bi, W.; Kong, T.; Qin, Q. Optical, photocatalytic properties of novel CuS nanoplate-based. *Cryst. Res. Technol.* **2009**, *44* (7), 729−735.
(26) Safrani, T.; Jopp, J.; Golan, Y. A comparative Study of the Structure and Optical Properties of Copper Sulfide thin films chemically deposited on various substrates. *RSC Adv.* **2013**, *3*, 23066−23074.
(27) Parker, G.; Hope, G. A.; Woods, R. Raman spectroscopic identification of surface species in the leaching of chalcopyrite. *Colloids Surf. A* **2008**, *318*, 160−168.
(28) Milekhin, A. G.; Yeryukov, N. A.; Sveshnikova, L. L.; Duda, T. A.; Kosolobov, S. S.; Latyshev, A. V.; Surovtsev, N. V.; Adichtchev, S. V.; Himcinschi, C.; Zenkevich, E. I.; et al. T. Raman scattering for probing semiconductor quantum dot arrays with a low areal density. *J. Phys. Chem. C* **2012**, *116*, 17164−17168.
(29) Hugall, J. T.; Baumberg, J. J.; Mahajan, S. Surface-enhanced Raman spectroscopy of CdSe quantum dots on nanostructured plasmonic surfaces. *Appl. Phys. Lett.* **2009**, *95*, 141111−1−3.
(30) Milekhin, A. G.; Yeryukov, N. A.; Sveshnikova, L. L.; Duda, T. A.; Zenkevich, E. I.; Kosolobov, S. S.; Latyshev, A. V.; Himcinschi, C.; Surovtsev, N. V.; Adichtchev, S. V.; Feng, Z. C.; et al. Surface Enhanced Raman Scattering of Light by ZnO Nanostructures. *J. Exp. Theor. Phys.* **2011**, *113*, 983−991.
(31) Milekhin, A. G.; Sveshnikova, L. L.; Duda, T. A.; Yeryukov, N. A.; Surovtsev, N. V.; Adichtchev, S. V.; Rodyakina, E. E.; Gutakovskii, A. K.; Latyshev, A. V.; Zahn, D. R. T. Surface-Enhanced Raman Scattering by Semiconductor Nanostructures. *Optoelectron., Instrum. Data Process.* **2013**, *5*, 504−513.
(32) Gutakovskii, A. K.; Sveshnikova, L. L.; Batsanov, S. A.; Yeryukov, N. A. Electron Microscopic Studies of CuS Nanocrystals Formed In Langmuir-Blodgett Films. *Optoelectron., Instrum. Data Process.* **2014**, *50*, 108−114.
(33) Powder diffraction file Inorganic Phase Alphabetical Index.: Ed. McClune W. F. International Centre for diffraction date, Swarthmore, USA 1984.
(34) Isac, L. A.; Duta, A.; Kriza, A.; Enesca, I. A.; Nanu, M. The growth of CuS thin films by Spray Pyrolysis. *J. Physics: Conf. Ser.* **2007**, *61*, 477−481.
(35) Ward, A. T. Raman Spectroscopy of Sulfur, Sulfur-Selenium, and Sulfur Arsenic Mixtures. *J. Phys. Chem.* **1968**, *72*, 4133−4139.
(36) Peiris, S. M.; Sweeney, J. S.; Campbell, A. J.; Heinz, D. L. Pressure-induced amorphization of covellite, CuS. *J. Chem. Phys.* **1996**, *104*, 11−16.
(37) Eckert, B.; Steudel, R. Molecular Spectra of Sulfur Molecules and Solid Sulfur Allotropes. *Top. Curr. Chem.* **2003**, *231*, 31−98.